



Published in final edited form as:

Langmuir. 2016 April 26; 32(16): 4043–4051. doi:10.1021/acs.langmuir.6b00560.

## Encapsulated Hydrogels by E-beam Lithography and Their Use in Enzyme Cascade Reactions

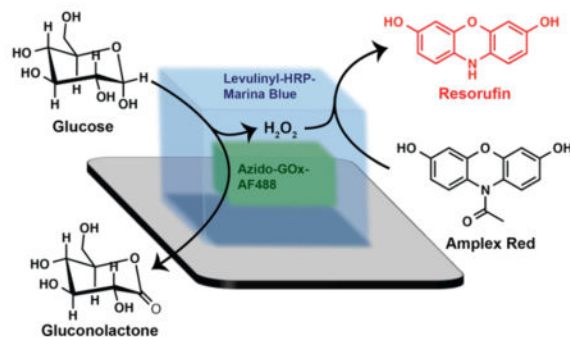
Rock J. Mancini<sup>†</sup>, Samantha J. Paluck, Erhan Bat<sup>‡</sup>, and Heather D. Maynard<sup>\*</sup>

Department of Chemistry and Biochemistry and California NanoSystems Institute, University of California, Los Angeles, 607 Charles E. Young Drive East, Los Angeles, California 90095-1569

### Abstract

Electron beam (e-beam) lithography was employed to prepare one protein encapsulated inside another by first fabricating protein-reactive hydrogels of orthogonal reactivity and subsequently conjugating the biomolecules. Exposure of thin films of eight arm star poly(ethylene glycol) (PEG) functionalized with biotin (**Biotin-PEG**), alkyne (**Alkyne-PEG**) or aminooxy (**AO-PEG**) end-groups to e-beam radiation resulted in cross-linked hydrogels with the respective functionality. It was determined via confocal microscopy that a nominal size exclusion effect exists for streptavidin immobilized on **Biotin-PEG** hydrogels of feature sizes ranging from 5 to 40  $\mu\text{m}$ . **AO-PEG** was subsequently patterned as an encapsulated core inside a contiguous outer shell of **Biotin-PEG**. Similarly, **Alkyne-PEG** was patterned as a core inside an **AO-PEG** shell. The hydrogel reactive end-groups were conjugated to dyes or proteins of complimentary reactivity, and the 3-D spatial orientation was determined for both configurations using confocal microscopy. The enzyme glucose oxidase (**GOX**) was immobilized in the core of the encapsulated **Alkyne-PEG** core/**AO-PEG** shell architecture, and horseradish peroxidase (**HRP**) was conjugated to the shell periphery. Bioactivity for the HRP-GOX enzyme pair was observed in this encapsulated configuration by demonstrating that the enzyme pair was capable of enzyme cascade reactions.

### Graphical Abstract



<sup>\*</sup>Corresponding Author: maynard@chem.ucla.edu.

<sup>†</sup>Department of Chemistry, Washington State University, 100 Dairy Road, Pullman Washington 99164-4630, USA

<sup>‡</sup>Present Address: Department of Chemical Engineering, Middle East Technical University, Ankara 06800, Turkey

## Introduction

Many approaches exist to generate micro or nano arrays of multiple proteins patterned within nano-scale proximity, including bias-assisted atomic force microscopy,<sup>1</sup> and electron beam (e-beam) lithography.<sup>2</sup> Several reports in particular, exploit electron beam radiation-induced cross-linking of poly(ethylene glycol) (PEG) and polymers of self assembled monolayers containing poly(ethylene glycols) to coat surfaces and form hydrogels features.<sup>3-13</sup> Also, hydrogel features have been fabricated by e-beam lithography for protein conjugation by utilizing linear and star PEGs with functional end groups.<sup>4,8,11,14</sup> It is proposed that the electron beams cause hydrogen abstraction and inter chain and chain-surface radical reactions forming cross-linked features on the surface with protein-reactive groups available for conjugation. By employing orthogonal reactive end-groups, different proteins can be patterned at the micron and nanometer size scale side-by-side. Using this approach, multiple types of polymers have also been patterned one on top of the other in a layered format with subsequent immobilization of the proteins.<sup>8,14</sup> However, the general interaction at the interface of these layers is as of yet unknown, and the formation of multilayers with subsequent three dimensional (3-D) characterization has not yet been reported.

Protein biochips, devices where multiple proteins are immobilized on a surface in close proximity, are becoming increasingly useful devices to study protein-protein interactions as well as for use in proteomics and biosensing.<sup>15</sup> Factors that affect the success of these surfaces include retention of protein activity after immobilization, density of immobilized proteins, and proximity of different proteins. Immobilizing proteins on surfaces initially focused on fabricating two-dimensional arrays through photoresist lithography, self-assembled monolayers, or tethering proteins to surface functionalities.<sup>16</sup> While these two-dimensional protein arrays provided new devices for biosensing, extending protein immobilization to include three-dimensional geometries at the micro and nano-scale could have many advantages including increased assay sensitivity and amount of immobilized protein. A three-dimensional configuration would also more closely resemble physiological interfaces. One way to obtain proteins in three-dimensional architectures is through encapsulation in gels. Many different proteins and enzymes have been immobilized or encapsulated in bulk gels for use in drug delivery,<sup>17</sup> tissue regeneration<sup>18</sup> and even in the food industry.<sup>19</sup> Additionally, electrospinning has been used to immobilize enzymes in three-dimensional networks.<sup>20</sup> While protein encapsulation in bulk gels is useful as a means for biomolecule delivery, precise control over protein positioning at the micro and nanometer scale is difficult. More recently researchers have been motivated to fabricate three-dimensional architectures on surfaces for protein encapsulation.

Immobilization of enzymes on surfaces and in bulk materials has largely been studied for use in proteomics and biosensing as well as to investigate protein-protein interactions. Enzymes have been encapsulated in hydrogels,<sup>21</sup> microgels,<sup>22</sup> sol-gels,<sup>23</sup> and patterned hydrogels<sup>24</sup> for applications ranging from monitoring molecular interactions to glucose sensing<sup>25,26</sup> and determination of oxidative stress.<sup>27</sup> More recently enzymes have been immobilized on fabricated surfaces prepared through hydrogel lithography,<sup>28</sup> photochemical based patterning,<sup>26,29</sup> e-beam lithography,<sup>30</sup> soft lithography<sup>31</sup> and 3-D printing<sup>32</sup> and have

been used in enzyme based assays. Methods for immobilization of enzymes in sequential layers, side by side or one on top of another have also been developed to further study enzyme activity on surfaces.<sup>26,33,34</sup>

Knowledge of the spatial orientation is useful because encapsulated architectures of PEG hydrogels fabricated by conventional UV photocross-linking have been used in conjunction with enzymes<sup>35</sup> and even whole cells.<sup>36</sup> Encapsulation increases the ratio of signal-to-noise and subsequent sensitivity<sup>35</sup> and also maintains viability of unique cell types such as islets of Langerhans.<sup>37,38</sup> While a myriad of immobilization strategies exist for the fabrication of biosensors,<sup>39</sup> some of the most common strategies used for PEG hydrogel surface arrays include avidin-biotin affinity,<sup>40–42</sup> oxime bond formation,<sup>43–45</sup> and 1,3 Huisgen cycloaddition.<sup>46–48</sup> Therefore, it would be useful to understand polymer distribution and permeability throughout PEG hydrogels, particularly in constructs with multiple instances of these protein conjugation strategies positioned in close proximity. As such, we sought to establish encapsulated hydrogel architectures patterned by e-beam lithography whereby a shell hydrogel forms a contiguous border in three dimensional space around an inner core hydrogel of orthogonal reactivity. This was accomplished by iterative patterning of different polymers (Figure 1) followed by immobilization of the proteins and investigation of activity.

## Experimental

### Materials

Synthesis for polymers (**Biotin-PEG**, **AO-PEG**, and **Alkyne-PEG**) as well as the modified enzymes azido glucose oxidase Alexa Fluor 488 conjugate (**Azide-GOX-AF488**) and levulinyl horseradish peroxidase marina blue conjugate (**Lev-HRP-MB**) can be found in the supporting information. Silicon wafers were purchased from University Wafers (Boston, MA). All other materials were purchased from Sigma Aldrich and utilized without further purification.

### Analytical Techniques

Silicon wafers were patterned with a JEOL 5910 scanning electron beam microscope. For multi-component PEGs, gold alignment features were fabricated on the silicon chips prior to PEG spin-coating and cross-linking. Pattern files were created in Design CAD 2000 and written with a JC Nability lithography system (Nanometer Pattern Generation System, Ver. 9.0). A Leica confocal SP2 1P microscope with fluorescence correlation spectroscopy was used for all confocal sectioning images. A Zeiss fluorescence microscope was used to observe 2-D pictures of immobilized enzymes, cross-reactivity controls, and evolution of resorufin through use of a transwell membrane.

### General e-beam Procedure

Exposure energies were empirically determined for all encapsulated microstructures by first independently optimizing the dose for each layer of polymer resists. Doses were varied in a linear gradient using area doses from 1 to 200  $\mu\text{C}/\text{cm}^2$  followed by visual inspection of the resulting hydrogels by bright-field microscopy. Minimal effective doses were used. Once these doses were determined, using a nano-realignment technique,<sup>8</sup> a second polymer resist

was cross-linked on top of the initial hydrogel layer and the optimization process was repeated. This process was repeated a third time to optimize the third layer thereby completing fabrication of the encapsulated hydrogel architecture. Defect rates in the final hydrogels were highly sensitive to the dose used, and typical hydrogels obtained are shown in all figures. Optimized doses for layers 2 and 3 were found to be approximately 50% of the optimal dose for a single layer.

#### **Fabrication of AO-PEG Encapsulated within Biotin-PEG (EA-1)**

**Biotin-PEG** (10  $\mu\text{L}$ , 1 wt% in MeOH) was spin coated onto a piranha cleaned silicon wafer with gold alignment marks (4000 rpm, 1 min). *Caution: Piranha solution reacts violently with organic materials.* The wafer was then patterned by e-beam lithography as an array of 40  $\mu\text{m}$  boxes (23 nm spot size, 30 kV accelerating voltage, 80  $\mu\text{C}/\text{cm}^2$  area dose). The wafer was developed by immersion in Milli-Q water for 30 seconds. The wafer was subsequently spin coated (4000 rpm, 1 min) with a solution of **AO-PEG** (10  $\mu\text{L}$ , 1 wt% in MeOH). The surface wafer was then re-aligned and patterned by e-beam lithography (23 nm spot size, 30 kV accelerating voltage, 40  $\mu\text{C}/\text{cm}^2$  area dose) as an array of 20  $\mu\text{m}$  boxes patterned in the center of the **Biotin-PEG**. The wafer was developed by immersion in Milli-Q water for 30 seconds. Next, the wafer was spin coated (4000 rpm, 1 min) with a third layer consisting of **Biotin-PEG** (10  $\mu\text{L}$ , 1 wt% in MeOH). The wafer was then realigned and patterned by e-beam lithography as an array of 40  $\mu\text{m}$  boxes (23 nm spot size, 30 kV accelerating voltage, 80  $\mu\text{C}/\text{cm}^2$  area dose). The wafer was developed by immersion in Milli-Q water for 30 seconds. Each fabrication step, including the final encapsulated hydrogel architecture (**EA-1**) was confirmed using an inverted bright-field microscope.

#### **Fabrication of Alkyne-PEG Encapsulated within AO-PEG (EA-2)**

**AO-PEG** (10  $\mu\text{L}$ , 1 wt% in MeOH) was spin coated onto a piranha cleaned silicon wafer with gold alignment marks (4000 rpm, 1 min). The wafer was then patterned by e-beam lithography as an array of 40  $\mu\text{m}$  boxes (23 nm spot size, 30 kV accelerating voltage, 40  $\mu\text{C}/\text{cm}^2$  area dose). The wafer was developed by immersion in Milli-Q water for 30 seconds. The wafer was subsequently spin coated (4000 rpm, 1 min) with a solution of **Alkyne-PEG** (10  $\mu\text{L}$ , 1 wt% in MeOH). The surface wafer was then realigned and patterned by e-beam lithography (23 nm spot size, 30 kV accelerating voltage, 20  $\mu\text{C}/\text{cm}^2$  area dose) as an array of 20  $\mu\text{m}$  boxes patterned in the center of the **AO-PEG**. The wafer was developed by immersion in Milli-Q water for 30 seconds. Next, the wafer was spin coated (4000 rpm, 1 min) with a third layer consisting of **AO-PEG** (10  $\mu\text{L}$ , 1 wt% in MeOH). The wafer was then realigned, patterned by e-beam lithography as an array of 40  $\mu\text{m}$  boxes (23 nm spot size, 30 kV accelerating voltage, 40  $\mu\text{C}/\text{cm}^2$  area dose), and developed by immersion in Milli-Q water for 30 seconds. Each lithography step, including fabrication of the final encapsulated hydrogel architecture (**EA-2**) was confirmed using an inverted bright-field microscope. Images shown in the paper that used **EA-2** architectures were produced via this procedure. We subsequently found that the same encapsulated structures can be fabricated more reliably by spin coating 1 wt% polymers in dichloroethane rather than methanol followed by e-beam lithography with dosages of 16  $\mu\text{C}/\text{cm}^2$  for the first PEG-AO layer, 2  $\mu\text{C}/\text{cm}^2$  for the PEG-alkyne layer and 12  $\mu\text{C}/\text{cm}^2$  for the second PEG-AO layer.

### Fluorophore Immobilization: AO-PEG Encapsulated within Biotin-PEG

The encapsulated hydrogel architecture **EA-1** was incubated with streptavidin Alexa Fluor 488 conjugate (0.1 mg/mL, 100 mM phosphate buffer, pH 7.0) for 1 h at room temperature before washing by immersion in Milli-Q water for 30 seconds. Next, the pattern was incubated with the aminoxy reactive dye, maleimide-coumarin (1.0 mg/mL in 10% DMSO<sub>(aq)</sub>) and 1% triethyl amine (TEA) for 1 h at room temperature before washing by immersion in 10% DMSO<sub>(aq)</sub> followed by Milli-Q water for 30 s each. The patterned hydrogel arrays were observed by confocal microscopy. The surface was illuminated using laser lines at 400 and 488 nm, and images were sectioned in the z dimension using a 100x oil objective advancing 400 nm with each section. Next, the focus of the microscope was shifted to approximately halfway through the microstructure. To confirm encapsulation, the 400 nm laser line was switched off and only the 488 nm line was used to illuminate a cross-section of the hydrogel architecture.

### Fluorophore Immobilization: Alkyne-PEG Encapsulated within AO-PEG

The encapsulated hydrogel architecture **EA-2** was incubated with Alexa Fluor-488 azide® (20  $\mu$ L, 1 mg/mL in DMSO), CuSO<sub>4</sub> (10  $\mu$ L, 1 mg/mL in 10% DMSO<sub>(aq)</sub>), and sodium ascorbate (10  $\mu$ L, 5 mg/mL in 10% DMSO<sub>(aq)</sub>) followed by washing by immersion first in 10% DMSO<sub>(aq)</sub> then in Milli-Q water for 30 seconds each. Next, **EA-2** was incubated with maleimide-coumarin dye (1 mg/mL in 10% DMSO<sub>(aq)</sub>) and 1% TEA for 1 h at room temperature in the dark before washing as above. Hydrogel arrays were observed by confocal microscopy using a 100x oil objective. Images were sectioned in the xy through z dimensions advancing 620 nm with each section. Images were also sectioned in the xz through y dimensions using similar sectioning parameters.

### Enzyme Immobilization in Encapsulated Hydrogels

The encapsulated architecture **EA-2** was exposed to **Lev-HRP-MB** in 40  $\mu$ L Dulbecco's Phosphate Buffered Saline (DPBS) at pH 7.4 for 3 h at room temperature followed by immersion in 5 mL aliquots of DPBS, pH 7.4, 5 times. Next, the surface was incubated with a solution of **Azide-GOX-AF488** (20  $\mu$ L, DPBS, pH 7.4), CuSO<sub>4</sub> (10  $\mu$ L, 1 mg/mL), and sodium ascorbate (10  $\mu$ L, 5 mg/mL) for 3 h at room temperature. The surface was washed by immersion in 10% DMSO in DPBS, pH 7.4, 3 times. Activity was assayed by adding the enzyme immobilized surface to a solution of glucose (10 mM) and Amplex Red (50  $\mu$ M) in DPBS, pH 7.4 and measuring the absorbance of resorufin at 560 nm after 2 h at 4°C.

## Results and Discussion

The protein-reactive polymers were prepared by modifying 8-arm star PEG polymers. Alkyne end-functionalized PEG polymer (**Alkyne-PEG**) was synthesized by reaction of the 8-arm amine-terminated PEG with the activated ester of pentynoic acid (see supporting information). Biotinylated 8-arm PEG (**Biotin-PEG**) was prepared from the corresponding amine PEG, and aminoxy PEG (**AO-PEG**) was obtained by reaction of hydroxyl terminated 8-arm PEG under Mitsunobu conditions with *N*-hydroxyphthalimide to produce PEG with aminoxy end-groups upon deprotection with hydrazine according to literature procedures.<sup>8,49</sup> Once polymers of orthogonal reactivity were obtained, the first parameter

investigated was protein distribution throughout PEG-hydrogel micro-patterns with varied feature sizes. Hydrogel arrays of a representative polymer, **Biotin-PEG**, were patterned by e-beam lithography ( $110 \mu\text{C}/\text{cm}^2$ ) to contain feature sizes ranging from 5 to 40  $\mu\text{m}$ . This polymer was chosen because of the strong binding with the protein streptavidin so that protein distribution could be readily observed. The patterns were subsequently incubated with a green fluorescent streptavidin (**SAv-AF488**) for 3 h at room temperature, and washed by immersion in DPBS, pH 7.4 for 5 minutes, three times. Confocal microscopy was performed using a 100x oil objective (full width at half max 640 nm) taking 400 nm sections in both z and y planes, thereby observing fluorescence of the micro-gel in three dimensions (Figure S4). The protein was found to be homogeneously dispersed throughout the microstructure for the 5  $\mu\text{m}$  feature size. As feature sizes increased, a decrease in fluorescence indicative of a slight size-exclusion effect was observed in the z-dimension for the center of the hydrogel feature relative to the edge. For the largest feature sizes (40  $\mu\text{m}$ ), increased fluorescence was found around the border of the hydrogel which may be attributed to the increase in height due to backscattered electrons as has been previously reported.<sup>4</sup>

Once the ability of proteins to penetrate to the core of hydrogel architectures was confirmed, fabrication of hydrogel architectures that contain two different polymers of orthogonal reactivity patterned in an encapsulated configuration was pursued next. The morphology of the polymer hydrogel along with localization of species conjugated to the polymer reactive end-groups in three dimensions was investigated. Fluorescent dyes and proteins were immobilized to demonstrate retention of bioactivity and to further investigate the permeability of the polymer hydrogels. Two different encapsulation strategies were employed: encapsulation of **AO-PEG** inside **Biotin-PEG** (**EA-1**) and encapsulation of **Alkyne-PEG** inside **AO-PEG** (**EA-2**).

The **AO-PEG** and **Biotin-PEG** polymers have a large difference in optimal reactive doses ( $80 \mu\text{C}/\text{cm}^2$  and  $110 \mu\text{C}/\text{cm}^2$  respectively); therefore, to prevent overexposure in subsequent lithographic steps, a reduced dose for each polymer was used. Encapsulated structures were fabricated over three patterning steps each consisting of spin coating a 1% methanolic solution of polymer (4000 rpm, 60 seconds), micro-alignment, e-beam lithography, and development by immersion in Milli-Q water. Thereby, a 40  $\mu\text{m}$  box of **Biotin-PEG** ( $60 \mu\text{C}/\text{cm}^2$ ) was patterned followed by a 20  $\mu\text{m}$  box of **AO-PEG** ( $40 \mu\text{C}/\text{cm}^2$ ) with a final 40  $\mu\text{m}$  box of **Biotin-PEG** ( $60 \mu\text{C}/\text{cm}^2$ ) patterned on top of the two preceding features to complete the encapsulated architecture (Figure 2a–b).

Next, distribution of polymer reactive end-groups within the encapsulated architectures was investigated. Fluorescent dyes were attached to the polymer end-groups retained in the hydrogel either through immobilization of fluorescent proteins or direct covalent attachment of the fluorophore. Specifically, **EA-1** was first exposed to Streptavidin-Alexa Fluor-488 (**SAv-AF488**) conjugate for 3 h at 4 °C followed by washing by immersion in Milli-Q water. The surfaces were then incubated with maleimide-coumarin (1 mg/mL in 10%  $\text{DMSO}_{(\text{aq})}$ ) in 1% TEA for 1 h at room temperature in the dark and washed in similar fashion thereby covalently attaching a blue coumarin dye to the aminoxy end-groups. Fluorescence of the hydrogel micro-patterns was observed, and the images were sectioned by confocal microscopy using a 100x oil objective to determine the reactive heterogeneity of

fluorophores immobilized within the polymer architecture (Figure 2). When the z-dimension was profiled to visualize the center of the hydrogel, the maximum intensity of the green channel was found to span the entire signal observed for the blue channel. We hypothesized that the green signal observed in the core of the hydrogel architecture was not a result of **Biotin-PEG**, but rather that this signal originated from coumarin fluorophore crosstalk. To test this, the microscope was focused at the midpoint in the z dimension through **EA-1**, and a fluorescence image was obtained in the x-y dimension only. In the first case, two laser lines were used. One laser line at 400 nm is strongly absorbed by the coumarin dye, and to a lesser extent Alexa Fluor 488. The second line at 488 nm is outside the absorption spectrum of coumarin and is therefore only absorbed by the Alexa Fluor 488. As expected, when both lasers were used to illuminate the sample, green fluorescence is clearly observed to envelop the coumarin fluorescence signal including the center of the structure. When only the 488 nm laser line is employed however, the green signal in the center of the structure is removed thereby revealing the location of maleimide-coumarin and SAv-488 dyes (Figure 2e–g). This result indicates that the blue maleimide-coumarin signal is encapsulated within the green SAv-488 fluorescence signal, and this may be correlated to polymer end-group reactivity to conclude that the **AO-PEG** is encapsulated as a core within an outer shell of **Biotin-PEG**.

Next **Alkyne-PEG** encapsulated within **AO-PEG** was investigated. Again to prevent overexposure in subsequent lithography steps, a reduced dose was used for each polymer. Encapsulated structures were fabricated utilizing similar conditions as before. A 40  $\mu\text{m}$  box of **AO-PEG** (40  $\mu\text{C}/\text{cm}^2$ ) was patterned followed by a 20  $\mu\text{m}$  box of **Alkyne-PEG** (15  $\mu\text{C}/\text{cm}^2$ ) with a third 40  $\mu\text{m}$  box of **AO-PEG** (40  $\mu\text{C}/\text{cm}^2$ ) patterned on top of the two preceding features (Figure 3a–c) to complete the second encapsulated architecture (**EA-2**) with morphology confirmed by bright-field microscopy (Figure S5). As an alternative, we found that more consistent patterns could be fabricated by spin coating polymer solutions dissolved in dichloroethane rather than methanol and also reducing the dosage of each layer (16  $\mu\text{C}/\text{cm}^2$  for the first **AO-PEG** layer, 2  $\mu\text{C}/\text{cm}^2$  for the **Alkyne-PEG** layer, and 12  $\mu\text{C}/\text{cm}^2$  for the top **AO-PEG** layer).

To investigate the distribution of polymer reactive end-groups in **EA-2**, the alkyne or aminoxy end-groups were covalently attached to fluorescent dyes of complimentary reactivity. In this case, the structure was first exposed to Alexa Fluor-488 azide<sup>®</sup> according to manufacturer instructions followed by washing by immersion in Milli-Q water. Next, **EA-2** was incubated with maleimide-coumarin (1 mg/mL in 10% DMSO<sub>(aq)</sub>) in 1% TEA for 1 hour at room temperature in the dark and washed in similar fashion. Fluorescent images of **EA-2** were sectioned by confocal microscopy using a 100x oil objective to determine the reactive heterogeneity of the **EA-2** polymer architecture (Figure 3). Via this method the **Alkyne-PEG** hydrogel (green) was present only within the contiguous shell of **AO-PEG** (blue) and cross-section analysis in the xy-z and xz-y dimensions confirmed the encapsulated architecture (Figure 3d–i and Figure 1e–f for additional images).

Once retention of polymer end-group reactivity was established, enzymes were immobilized in the **EA-2** encapsulated configuration. Horseradish peroxidase (HRP) and glucose oxidase (GOX) were chosen because they have been used previously to effect enzyme cascade reactions when contained in polymersomes.<sup>50,51</sup> Thus, HRP and GOX were functionalized

with levulinyl or azido moieties, respectively, for fabrication of GOX immobilized as a core encapsulated by a HRP shell using the **EA-2** architecture. Azide modification was chosen for GOX as several azides are known inhibitors of HRP.<sup>52</sup> Therefore, GOX was modified to contain free azide moieties through a modification of the reported procedure with imidazole-1-sulfonyl azide hydrochloride,<sup>53,54</sup> using 3 equivalents of the diazo transfer reagent. Upon purification by centriprep ultra-centrifugation (MWCO 3 kDa), the protein conjugate was assayed for azide moieties by reaction with Alexa Fluor 594 Click It® alkyne. Degree of labeling determined by UV absorbance at 280 nm (protein) and 590 nm (dye) was found to be 1.4 azides per GOX protein. Likewise, HRP was modified to contain levulinyl moieties via incubation with *N*-hydroxy succinimidyl levulinate (3 eq, DPBS, 3 h, rt) and purified by centriprep (MWCO 3 kDa).<sup>55</sup> The conjugate was assayed for free ketones by reaction with Alexa Fluor 488® hydrazide under reducing conditions with NaBH<sub>3</sub>CN. Degree of labeling determined by UV absorbance at 280 nm (protein) and 490 nm (dye) was found to be 1.0 hydrazide reactive moieties per HRP protein. For details of protein modification and characterization, see the supporting information.

Fluorophore selection for the immobilized conjugates was found to be non-trivial. Specifically, GOX contains a flavin adenine dinucleotide redox cofactor with strong absorption in the blue region. These findings necessitate that for a blue/green pair of fluorophores, GOX be labeled green with HRP labeled as blue. Furthermore, when a protein encapsulated in the core contains a fluorophore with emission in the absorption range of the shell fluorophore, significant crosstalk was observed between fluorophores as demonstrated with **EA-1** described above. Therefore, azide modified GOX and levulinyl modified HRP were made fluorescent by incubation with TFP-Alexa Fluor 488® and Marina Blue® NHS ester to produce the fluorescent protein conjugates **Azide-GOX-AF488** and **Lev-HRP-MB**, respectively. Degree of labeling studies were conducted by UV absorbance and it was found that **Azide-GOX-AF488** contained 0.7 fluorophores per protein (280 nm protein, 490 nm dye) and 0.68 fluorophores per protein was observed for **Lev-HRP-MB** (280 nm protein, 350 nm dye). Modification with the functional group and dyes decreased the native activity of both proteins to 32% for **Lev-HRP-MB** and 53% for **Azide-GOX-AF488** (Figure S6).

Multi-component hydrogels were fabricated as before to contain an **Alkyne-PEG** hydrogel core encapsulated within an **AO-PEG** shell (**EA-2**). The microstructure was then incubated with **Lev-HRP-MB** for 24 h at 4°C. The surfaces were washed with DPBS before exposure to **Azide-GOX-AF488**, CuSO<sub>4</sub>, and sodium ascorbate in DPBS for 24 hours at 4°C. The surfaces were washed again with reaction buffer and the rinsing solutions from each wash cycle were assayed for enzyme activity with no activity detectable after 3 washes. The immobilized enzymes were then viewed by fluorescence microscopy (Figure S7). Furthermore, chemical immobilization and cross reactivity was probed by fabrication of a wafer to contain **Alkyne-PEG** patterned next to **AO-PEG**. This wafer was incubated as before with **Azide-GOX-AF488**, CuSO<sub>4</sub>, and sodium ascorbate in DPBS for 24 hours at 4°C. The surface was washed 5 times with reaction buffer and viewed by fluorescence microscopy. As expected a large fluorescence signal was present within the **Alkyne-PEG** hydrogel with only minimal fluorescence detected from the **AO-PEG** hydrogel (Figure S8).

Enzyme activity was then confirmed through an enzyme cascade reaction between HRP and GOX. When hydrogen peroxide is present, HRP can modify numerous substrates in solution<sup>56,57</sup> including fluorescent substrates<sup>58–63</sup> and Amplex Red®. This reporter molecule may be used to quantify enzymatic activity or hydrogen peroxide concentration.<sup>64</sup>

Additionally, GOX is known to liberate hydrogen peroxide as a byproduct in the conversion of glucose to gluconic acid.<sup>65,66</sup> It has been shown that glucose and GOX coupled with a fluorescent HRP substrate and HRP may be used to probe activity of the enzyme pair as glucose oxidation by GOX provides one of the substrates (hydrogen peroxide) required for HRP activity.<sup>67,68</sup>

First, control experiments were conducted (see supporting information for fabrication of controls). Surfaces with no patterns or patterns of unfunctionalized PEG-OH were incubated with both enzymes under identical conditions. These surfaces were then washed in identical fashion to **EA-2** and exposed to a solution that included substrates for both enzymes (glucose, 10 mM, hydrogen peroxide, 300 ppm, and Amplex Red, 50  $\mu$ M). In a separate experiment, **Azide-GOX-AF488** was immobilized alone on a surface of **Alkyne-PEG**. To do this, **Alkyne-PEG** hydrogel arrays were fabricated by e-beam lithography and **Azide-GOX-AF488** was immobilized on the patterns using conditions identical to immobilization of the enzyme in **EA-2**. The surface immobilized **Azide-GOX-AF488** was then incubated with a solution of glucose substrate along with **Lev-HRP-MB** (1  $\mu$ g/mL) and Amplex Red (50  $\mu$ M). In addition, **Lev-HRP-MB** was immobilized alone on a surface of **AO-PEG**. This was achieved by fabricating patterns of **AO-PEG** and incubating with **Lev-HRP-MB** in identical fashion to **EA-2**. The surface was then exposed to both substrates for HRP (Amplex Red and hydrogen peroxide at the same concentration). Evolution of resorufin in all samples was measured after 2 h and the results were compared relative to **Lev-HRP-MB** activity when immobilized alone (Figure 4b).

Although by visual inspection, protein was clearly observed to adsorb onto the surface of the bare silicon substrate, lack of enzymatic activity in this experiment (0.5%, Figure 4b) indicated that non-specific adsorption to the surface inactivates both enzymes. Additionally, wash solutions from the bare silicon surface were assayed for activity, and no activity was detectable after 3 wash cycles (out of 5 performed) indicating that active enzymes were not present in or diffusing into the final wash solution. This implies that all enzyme activity in subsequent experiments is a result of enzymes present in the PEG hydrogels. For unmodified PEG-OH hydrogels, a minimal level of enzyme activity (13%) was observed after washing. This was likely due to enzymes that diffused into the PEG-OH hydrogel array and not covalently immobilized, yet also not removed during the wash steps. When **Lev-HRP-MB** or **Azide-GOX-AF488** were immobilized alone and incubated with appropriate substrates and partner enzymes in solution, resorufin was evolved similarly, as expected. This demonstrated that the proteins singly immobilized within the gels were still active.

Finally, activity retention was confirmed for both enzymes in the encapsulated format by effecting an enzyme cascade reaction with glucose and Amplex Red® substrates with both enzymes immobilized (Figure 4a). The **EA-2** GOX encapsulated within HRP patterned surfaces were incubated with glucose (10 mM) and Amplex Red (50  $\mu$ M) substrates at 4°C, and fluorescence of resorufin was measured after 2 hours. To visualize resorufin emanating

from **EA-2** in real-time, the silicon wafer containing the microstructure was mounted on a trans-well membrane and exposed to glucose (10 mM) and Amplex Red (50  $\mu$ M) while viewing by fluorescence microscopy. The red color of the resorufin was clearly observed (Figure 4c and Figure S9). The encapsulated surface with immobilized enzymes **Azide-GOX-AF488** and **Lev-HRP-MB** displayed activity similar to **Lev-HRP-MB** and **Azide-GOX-AF488** immobilized alone. However, there cannot be a direct quantitative comparison since the first is a three layered format system and the others are single hydrogel features with the partner protein in solution. Yet, the data demonstrates that the glucose was able to diffuse to the GOX core and the resulting hydrogen peroxide to the HRP periphery to convert Amplex Red to resorufin. The data also demonstrates that both proteins remain active in the encapsulated architecture.

## Conclusions

PEG hydrogel microstructures were fabricated by e-beam lithography such that functionalized protein-reactive PEG was patterned as a core, encapsulated within a contiguous shell comprised of PEG with orthogonal reactivity. The reactive heterogeneity of multi-component PEG-based hydrogels was demonstrated by confocal microscopy after fluorescent dyes were conjugated to the polymers. The enzymes glucose oxidase and horseradish peroxidase were functionalized with fluorophores and complimentary reactivity relative to the PEG hydrogel end-groups. Both enzymes were immobilized in an encapsulated configuration. The encapsulated enzymes exhibit reactivity demonstrating enzyme cascades are possible within the encapsulated hydrogel architectures.

## Supplementary Material

Refer to Web version on PubMed Central for supplementary material.

## Acknowledgments

This work was supported by funds from the National Science Foundation through the Center for Scalable and Integrated NanoManufacturing (SINAM, CMMI-0751621). RJM thanks the NSF and California NanoSystems Institute for a Materials Creation Training Program Fellowship. SJP thanks the NIH Chemistry Biology Interface Training Fellowship (T32 GM 008496) and UCLA Graduate Division for funding. E.B. thanks the Netherlands Organization for Scientific Research and Marie Curie Cofund Action for the financial support (Rubicon Grant 680-50-1101).

## References

1. Xing CY, Zheng ZK, Zhang BL, Tang JL. Nanoscale patterning of multicomponent proteins by bias-assisted atomic force microscopy nanolithography. *Chem Phys Chem*. 2011; 12:1262–1265. [PubMed: 21425234]
2. Kolodziej CM, Maynard HD. Electron-beam lithography for patterning biomolecules at the micron and nanometer scale. *Chem Mater*. 2012; 24:774–780.
3. Sofia SJM, EW. Grafting of PEO to polymer surfaces using electron beam irradiation. *J Biomed Mater Res*. 1998; 40:153–163. [PubMed: 9511110]
4. Krsko P, Sukhishvili S, Mansfield M, Clancy R, Libera M. Electron-beam surface-patterned poly(ethylene glycol) microhydrogels. *Langmuir*. 2003; 19:5618–5625.
5. Hong Y, Krsko P, Libera M. Protein surface patterning using nanoscale PEG hydrogels. *Langmuir*. 2004; 20:11123–11126. [PubMed: 15568866]

6. Rundqvist J, Hoh JH, Haviland DB. Directed immobilization of protein-coated nanospheres to nanometer-scale patterns fabricated by electron beam lithography of poly(ethylene glycol) self-assembled monolayers. *Langmuir*. 2006; 22:5100–5107. [PubMed: 16700600]
7. Saaem I, Papasotiropoulos V, Wang T, Soteropoulos P, Libera MJ. Hydrogel-based protein nanoarrays. *J Nanosci Nanotechnol*. 2007; 7:2623–2632. [PubMed: 17685276]
8. Christman KL, Schopf E, Broyer RM, Li RC, Chen Y, Maynard HD. Protein nanopatterns by oxime bond formation. *Langmuir*. 2011; 27:1415–1418. [PubMed: 21192671]
9. Krsko P, Kaplan JB, Libera M. Spatially controlled bacterial adhesion using surface-patterned poly(ethylene glycol) hydrogels. *Acta Biomater*. 2009; 5:589–596. [PubMed: 18842467]
10. Misuk B, Gemeinhart RA, Divan R, Suthar KJ, Mancini DC. Fabrication of poly(ethylene glycol) hydrogel structures for pharmaceutical applications using electron beam and optical lithography. *J Vac Sci Technol B, Microelectron Nanometer Struct*. 2010; 28:24–29.
11. Christman KL, Broyer RM, Schopf E, Kolodziej CM, Chen Y, Maynard HD. Protein nanopatterns by oxime bond formation. *Langmuir*. 2011; 27:1415–1418. [PubMed: 21192671]
12. Kolodziej CM, Maynard HD. Shape-shifting micro- and nanopatterns controlled by temperature. *J Am Chem Soc*. 2012; 134:12386–12389. [PubMed: 22803698]
13. Bat E, Lin EW, Saxer S, Maynard HD. Morphing hydrogel patterns by thermo-reversible fluorescence switching. *Macromol Rapid Commun*. 2014; 35:1260–1265. [PubMed: 24740924]
14. Broyer RM, Schopf E, Kolodziej CM, Chen Y, Maynard HD. Dual click reactions to micropattern proteins. *Soft Matter*. 2011; 7:9972–9977.
15. Rusmini F, Zhong Z, Feijen J. Protein immobilization strategies for protein biochips. *Biomacromolecules*. 2007; 8:1775–1789. [PubMed: 17444679]
16. Blawas AS, Reichert WM. Protein patterning. *Biomaterials*. 1998; 19:595–609. [PubMed: 9663732]
17. Hoare TR, Kohane DS. Hydrogels in drug delivery: progress and challenges. *Polymer*. 2008; 49:1993–2007.
18. Slaughter BV, Khurshid SS, Fisher OZ, Khademhosseini A, Peppas NA. Hydrogels in regenerative medicine. *Adv Mater*. 2009; 21:3307–3329. [PubMed: 20882499]
19. Gibbs BF, Kermasha S, Alli I, Mulligan CN. Encapsulation in the food industry: a review. *Int J Food Sci Nutr*. 1999; 50:213–224. [PubMed: 10627837]
20. Wang ZG, Wan LS, Liu ZM, Huang XJ, Xu ZK. Enzyme immobilization on electrospun polymer nanofibers: An overview. *J Mol Catal B: Enzym*. 2009; 56:189–195.
21. Feng L, Wang L, Hu Z, Tian Y, Xian Y, Jin L. Encapsulation of horseradish peroxidase into hydrogel, and its bioelectrochemistry. *Microchim Acta*. 2009; 164:49–54.
22. Schachschaal S, Adler HJ, Pich A, Wetzel S, Matura A, van Pee KH. Encapsulation of enzymes in microgels by polymerization/cross-linking in aqueous droplets. *Colloid Polym Sci*. 2011; 289:693–698.
23. Avnir D, Braun S, Lev O, Ottolenghi M. Enzymes and other proteins entrapped in sol-gel materials. *Chem Mater*. 1994; 6:1605–1614.
24. Dominguez MM, Wathier M, Grinstaff MW, Schaus SE. Immobilized hydrogels for screening of molecular interactions. *Anal Chem*. 2007; 79:1064–1066. [PubMed: 17263336]
25. Liu BH, Hu RQ, Deng JQ. Characterization of immobilization of an enzyme in a modified Y zeolite matrix and its application to an amperometric glucose biosensor. *Anal Chem*. 1997; 69:2343–2348. [PubMed: 9212705]
26. Kim DN, Lee W, Koh WG. Micropatterning of proteins on the surface of three-dimensional poly(ethylene glycol) hydrogel microstructures. *Anal Chim Acta*. 2008; 609:59–65. [PubMed: 18243874]
27. Kim SH, Kim B, Yadavalli VK, Pishko MV. Encapsulation of enzymes within polymer spheres to create optical nanosensors for oxidative stress. *Anal Chem*. 2005; 77:6828–6833. [PubMed: 16255579]
28. Lee Y, Lee HJ, Son KJ, Koh WG. Fabrication of hydrogel-micropatterned nanofibers for highly sensitive microarray-based immunosensors having additional enzyme-based sensing capability. *J Mater Chem*. 2011; 21:4476–4483.

29. Larsen EKU, Mikkelsen MBL, Larsen NB. Facile photoimmobilization of proteins onto low-binding PEG-coated polymer surfaces. *Biomacromolecules*. 2014; 15:894–899. [PubMed: 24524417]
30. Tudorache M, Mahalu D, Teodorescu C, Stan R, Bala C, Parvulescu VI. Biocatalytic microreactor incorporating HRP anchored on micro-/nano-lithographic patterns for flow oxidation of phenols. *J Mol Catal B: Enzym*. 2011; 69:133–139.
31. Wilhelm T, Wittstock G. Generation of periodic enzyme patterns by soft lithography and activity imaging by scanning electrochemical microscopy. *Langmuir*. 2002; 18:9485–9493.
32. Gupta MK, Meng F, Johnson BN, Kong YL, Tian L, Yeh YW, Masters N, Singamaneni S, McAlpine MC. 3D printed programmable release capsules. *Nano Lett*. 2015; 15:5321–5329. [PubMed: 26042472]
33. Jang CH, Stevens BD, Phillips R, Calter MA, Ducker WA. A strategy for the sequential patterning of proteins:3 catalytically active multiprotein nanofabrication. *Nano Lett*. 2003; 3:691–694.
34. Jang CH, Stevens BD, Carlier PR, Calter MA, Ducker WA. Immobilized enzymes as catalytically-active tools for nanofabrication. *J Am Chem Soc*. 2002; 124:12114–12115. [PubMed: 12371849]
35. Russell RJ, Pishko MV, Simonian AL, Wild JR. Poly(ethylene glycol) hydrogel-encapsulated fluorophore-enzyme conjugates for direct detection of organophosphorus neurotoxins. *Anal Chem*. 1999; 71:4909–4912. [PubMed: 10565282]
36. Koh WG, Revzin A, Pishko MV. Poly(ethylene glycol) hydrogel microstructures encapsulating living cells. *Langmuir*. 2002; 18:2459–2462. [PubMed: 12088033]
37. Cruise GM, Hegre OD, Scharp DS, Hubbell JA. A sensitivity study of the key parameters in the interfacial photopolymerization of poly(ethylene glycol) diacrylate upon porcine islets. *Biotechnol Bioeng*. 1998; 57:655–665. [PubMed: 10099245]
38. Pathak CP, Sawhney AS, Hubbell JA. Rapid photopolymerization of immunoprotective gels in contact with cells and tissue. *J Am Chem Soc*. 1992; 114:8311–8312.
39. Sassolas A, Blum LJ, Leca-Bouvier BD. Immobilization strategies to develop enzymatic biosensors. *Biotechnol Adv*. 2012; 30:489–511. [PubMed: 21951558]
40. Weber PC, Ohlendorf DH, Wendoloski JJ, Salemme FR. Structural origins of high-affinity biotin binding to streptavidin. *Science*. 1989; 243:85–88. [PubMed: 2911722]
41. Dai X, Yang W, Firlar E, Marras SAE, Libera M. Surface-patterned microgel-tethered molecular beacons. *Soft Matter*. 2012; 8:3067–3076.
42. Hyun J, Ahn SJ, Lee WK, Chilkoti A, Zauscher S. Molecular recognition-mediated fabrication of protein nanostructures by dip-pen lithography. *Nano Lett*. 2002; 2:1203–1207.
43. Boncheva M, Scheibler L, Lincoln P, Vogel H, Akerman B. Design of oligonucleotide arrays at interfaces. *Langmuir*. 1999; 15:4317–4320.
44. Mancini RJ, Li RC, Tolstyka ZP, Maynard HD. Synthesis of a photo-caged aminoxy alkane thiol. *Org Biomol Chem*. 2009; 7:4954–4959. [PubMed: 19907786]
45. Falsey JR, Renil M, Park S, Li SJ, Lam KS. Peptide and small molecule microarray for high throughput cell adhesion and functional assays. *Bioconjugate Chem*. 2001; 12:346–353.
46. Duckworth BP, Xu JH, Taton TA, Guo A, Distefano MD. Site-specific, covalent attachment of proteins to a solid surface. *Bioconjugate Chem*. 2006; 17:967–974.
47. Chelmoski R, Koster SD, Kerstan A, Prekelt A, Grunwald C, Winkler T, Metzler-Nolte N, Terfort A, Woll C. Peptide-based SAMs that resist the adsorption of proteins. *J Am Chem Soc*. 2008; 130:14952–14953. [PubMed: 18928285]
48. Chevlot Y, Bouillon C, Vidal S, Morvan F, Meyer A, Cloarec JP, Jochum A, Praly JP, Vasseur JJ, Souteyrand E. DNA-based carbohydrate biochips: A platform for surface glyco-engineering. *Angew Chem Int Ed*. 2007; 46:2398–2402.
49. Schlick TL, Ding ZB, Kovacs EW, Francis MB. Dual-surface modification of the tobacco mosaic virus. *J Am Chem Soc*. 2005; 127:3718–3723. [PubMed: 15771505]
50. van Dongen SFM, Nallani M, Cornelissen J, Nolte RJM, van Hest JCM. Three-enzyme cascade reaction through positional assembly of enzymes in a polymersome nanoreactor. *Chem Eur J*. 2009; 15:1107–1114. [PubMed: 19072950]

51. Vriezema DM, Garcia PML, Oltra NS, Hatzakis NS, Kuiper SM, Nolte RJM, Rowan AE, van Hest JCM. Positional assembly of enzymes in polymersome nanoreactors for cascade reactions. *Angew Chem Int Ed.* 2007; 46:7378–7382.
52. Liu G, Amin S, Okuhama NN, Liao G, Mingle LA. A quantitative evaluation of peroxidase inhibitors for tyramide signal amplification mediated cytochemistry and histochemistry. *Histochem Cell Biol.* 2006; 126:283–291. [PubMed: 16508759]
53. van Dongen SFM, Teeuwen RLM, Nallani M, van Berkel SS, Cornelissen J, Nolte RJM, van Hest JCM. Single-step azide introduction in proteins via an aqueous diazo transfer. *Bioconjugate Chem.* 2009; 20:20–23.
54. Goddard-Borger ED, Stick RV. An efficient, inexpensive, and shelf-stable diazotransfer reagent: Imidazole-1-sulfonyl azide hydrochloride. *Organic Letters.* 2007; 9:3797–3800. [PubMed: 17713918]
55. Heredia KL, Tolstyka ZP, Maynard HD. Aminooxy end-functionalized polymers synthesized by ATRP for chemoselective conjugation to proteins. *Macromolecules.* 2007; 40:4772–4779.
56. Zaitso K, Ohkura Y. *Analytical Biochemistry.* 1980; 109:109. [PubMed: 7469007]
57. Marklund S, Ohlsson PI, Opara A, Paul KG. Substrate profiles of acidic and slightly basic horseradish peroxidases. *Biochim Biophys Acta.* 1974; 350:304–313. [PubMed: 4847564]
58. Rota C, Chignell CF, Mason RP. Evidence for free radical formation during the oxidation of 2'-7'-dichlorofluorescein to the fluorescent dye 2'-7'-dichlorofluorescein by horseradish peroxidase: Possible implications for oxidative stress measurements. *Free Radic Biol Med.* 1999; 27:873–881. [PubMed: 10515592]
59. Odo J, Sogawa Y, Inoguchi M, Hirai A. Fluorescent derivatization of xanthurenic acid and nicotinic acid with horseradish peroxidase in the presence of excess hydrogen peroxide. *Anal Sci.* 2011; 27:105–109. [PubMed: 21233570]
60. vanGijlswijk RPM, Wiegant J, Vervenne R, Lasan R, Tanke HJ, Raap AK. Horseradish peroxidase-labeled oligonucleotides and fluorescent tyramides for rapid detection of chromosome-specific repeat sequences. *Cytogenet Genome Res.* 1996; 75:258–262.
61. Rota C, Fann YC, Mason RP. Phenoxyl free radical formation during the oxidation of the fluorescent dye 2',7'-dichlorofluorescein by horseradish peroxidase - Possible consequences for oxidative stress measurements. *J Biol Chem.* 1999; 274:28161–28168. [PubMed: 10497168]
62. Hollis TM, Katora ME, Montini J. A simple fluorescent method for simultaneous determination of aortic permeability to horseradish-peroxidase and bovine serum-albumin. *J Histochem Cytochem.* 1981; 29:1405–1410. [PubMed: 6798104]
63. Yang HH, Li DH, Chen XL, Qu HY, Ding MT, Xu JG. Tetra-substituted amino aluminum phthalocyanine as a new red-region fluorescent substrate for horseradish peroxidase based enzyme-linked immunosorbent assay. *Chin J Chem.* 2002; 20:1573–1578.
64. Mishin V, Gray JP, Heck DE, Laskin DL, Laskin JD. Application of the Amplex red/horseradish peroxidase assay to measure hydrogen peroxide generation by recombinant microsomal enzymes. *Free Radic Biol Med.* 2010; 48:1485–1491. [PubMed: 20188819]
65. Kleppe K. Effect of hydrogen peroxide on glucose oxidase from aspergillus niger. *Biochem.* 1966; 5:139–143. [PubMed: 5938931]
66. Wu M, Lin ZH, Schaferling M, Durkop A, Wolfbeis OS. Fluorescence imaging of the activity of glucose oxidase using a hydrogen-peroxide-sensitive europium probe. *Anal Biochem.* 2005; 340:66–73. [PubMed: 15802131]
67. Schroder M, Friedl P. Enzymatic determination of D-glucose in cell culture media using glucose oxidase, horseradish peroxidase and 3,3',5,5'-tetramethylbenzidine. *Gen Eng Biotechnol.* 1997; 17:157–163.
68. Segawa T, Kakizaki A, Kamidate T, Watanabe H. Fluorescein chemiluminescent assay of glucose in serum using glucose-oxidase and horseradish-peroxidase. *Anal Sci.* 1992; 8:785–788.

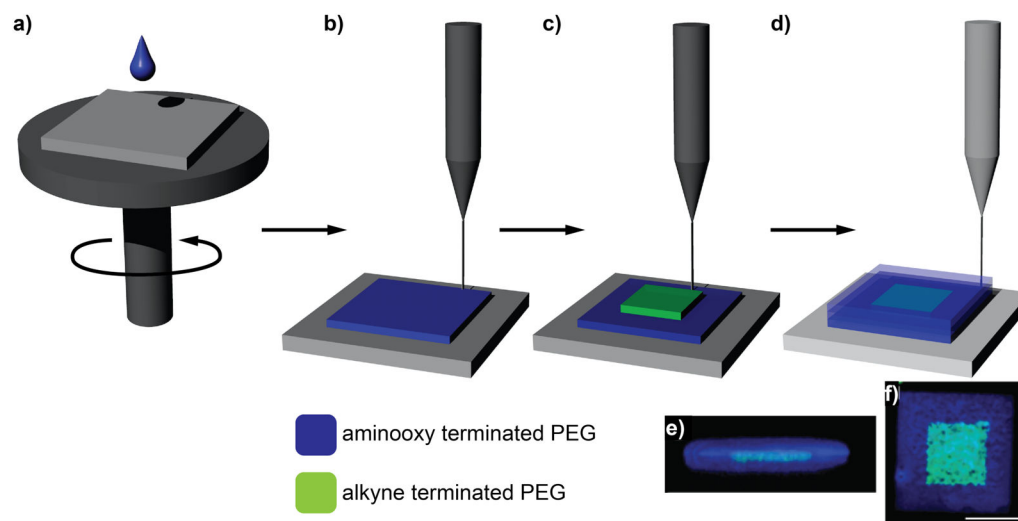


**Figure 1.**

Fabrication of an encapsulated PEG hydrogel by e-beam lithography. a) A methanolic solution of **AO-PEG** is spin coated onto a silicon substrate before b) crosslinking by exposure to e-beam and removal of unreacted polymer by developing in Milli-Q water. The process is then repeated first c) with a polymer of orthogonal reactivity (**Alkyne-PEG**) followed by d) capping with the original polymer of **AO-PEG**. Maximum transparency projection in e) xy-z and f) xz-y space of the **Alkyne-PEG** core stained with Alexa-488 Azide (green) patterned inside a contiguous shell of **AO-PEG** stained with maleimide functionalized coumarin (blue) as sectioned by confocal microscopy. Scale bar is 20  $\mu\text{m}$ .

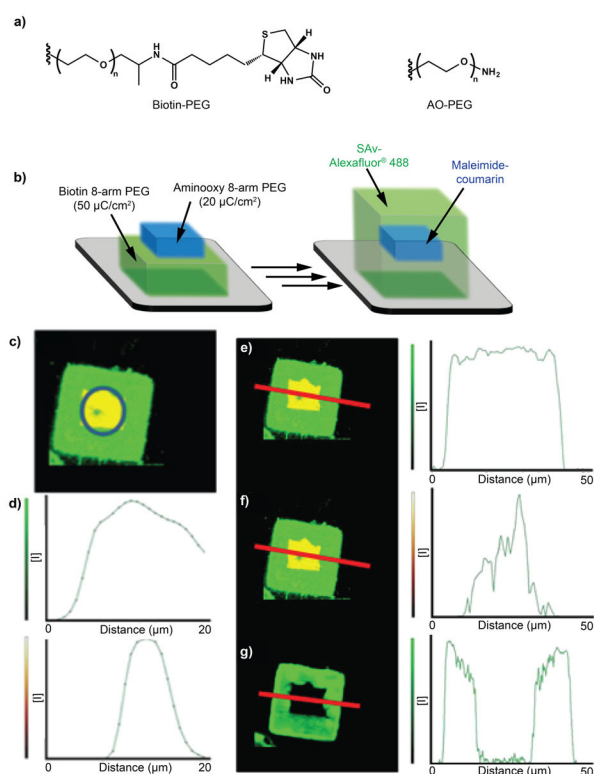


**Figure 2.**

Reactive heterogeneity of the polymer architecture with a) biotin and aminoxy end-groups was investigated by b) first patterning **AO-PEG** on top of a **Biotin-PEG** hydrogel before completing the encapsulated architecture with a second layer of **Biotin-PEG**. Subsequent staining with streptavidin-Alexa Fluor 488 conjugate (green) followed by maleimide-coumarin (blue) allowed for c) fluorescence imaging by confocal microscopy (blue maleimide-coumarin has been digitally replaced with yellow coloring for clarity) with d) profiles through the center of the microstructure in the z dimension (blue circle) confirming encapsulation as the maximum intensity of the green channel (top) completely surrounds the maximum intensity of the blue channel (bottom). Fluorescence image and profile in the x-y dimension approximately halfway through the microstructure (red line) of **AO-PEG** encapsulated within **Biotin-PEG** with pronounced signals in both the e) green and f) blue channels when the substrate is simultaneously illuminated with laser wavelengths at 400 (coumarin absorbance) and 490 nm (Alexa Fluor 488 absorbance). g) Fluorescence in the **AO-PEG** core is no longer observed when the sample is only illuminated with the 490 nm laser line.

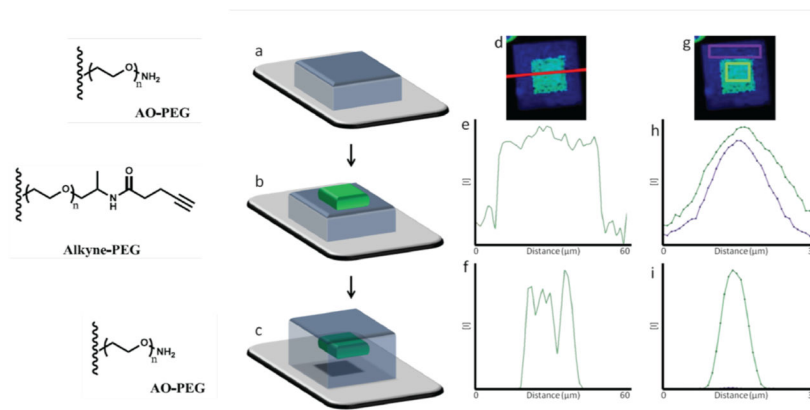


**Figure 3.** Fabrication of an encapsulated micro-pattern achieved by a) patterning a 40  $\mu\text{m}$  box consisting of **AO-PEG** hydrogel, development and realignment to pattern b) a 20  $\mu\text{m}$  box of **alkyne-PEG** on top of the existing microstructure. c) Subsequent capping with an additional layer of **AO-PEG** patterned as a 40  $\mu\text{m}$  box completed encapsulation. Microstructures were stained with maleimide-coumarin (blue) and Alexa Fluor-488 Azide (green) before measurement of the fluorescence profile of the d) xy-through z maximum fluorescence projection with e) blue and f) green channels. Confocal slices were obtained in the z direction with g) z-profiles in the center and on the border of the microstructure. h) The blue channel fluorescence was found to surround a contiguous border of the i) green channel fluorescence.

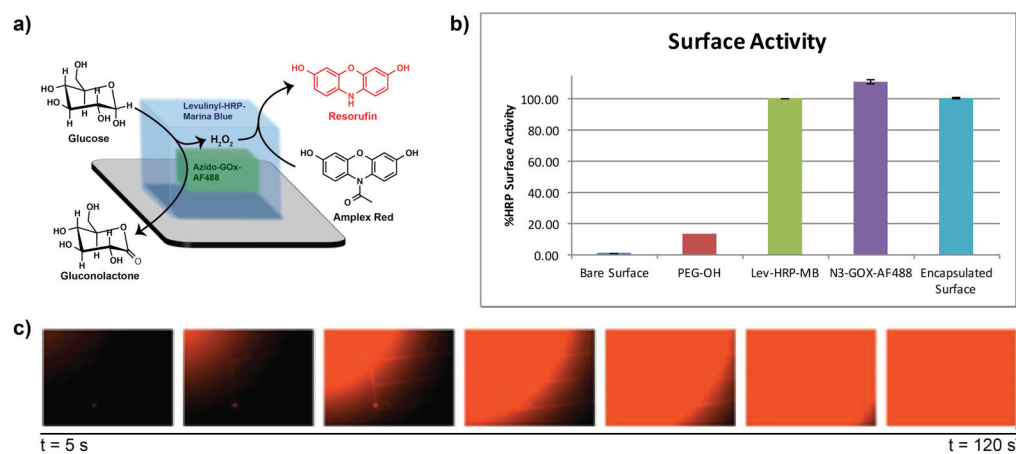


**Figure 4.**

a) Enzyme cascade between **Azide-GOX-AF488** and **Lev-HRP-MB** in an encapsulated hydrogel. b) Surface activity of **EA-2** and relative to control surfaces. Surfaces were compared relative to Lev-HRP-MB substrate (set to 100%). Error bars represent the standard deviation of measurements performed in triplicate for the same surface (for all but PEG-OH which was conducted once). c) Time-lapse pictures of resorufin emanating from enzymes immobilized on a multi-component hydrogel with encapsulated architecture were obtained by performing the enzyme cascade experiment as described above with the surface mounted on a trans-well membrane.